JGR Atmospheres

RESEARCH ARTICLE
10.1029/2021JD035478

Size Distribution of Mineral Dust Emissions From Sparsely Vegetated and Supply-Limited Dryland Soils

Nicholas P. Webb[1], Sandra L. LeGrand[2], Brad F. Cooper[1], Ericha M. Courtright[1], Brandon L. Edwards[1], Christopher Felt[2], Justin W. Van Zee[1], and Nancy P. Ziegler[2]

[1]USDA-ARS Jornada Experimental Range, Las Cruces, NM, USA, [2]US Army Engineer Research and Development Center, Cold Regions Research and Engineering Laboratory (CRREL), Hanover, NH, USA

Key Points:

- Dust emission flux particle size distribution is dependent on wind friction velocity over vegetated and crusted dryland soils
- Dust emission flux is enriched in fine (<5 μm) particles with increasing wind friction velocity
- Dust emission models need to represent variability in dust particle size distribution from sediment supply-limited aeolian systems

Supporting Information:

Supporting Information may be found in the online version of this article.

Correspondence to:

N. P. Webb,
nwebb@nmsu.edu

Citation:

Webb, N. P., LeGrand, S. L., Cooper, B. F., Courtright, E. M., Edwards, B. L., Felt, C., et al. (2021). Size distribution of mineral dust emissions from sparsely vegetated and supply-limited dryland soils. *Journal of Geophysical Research: Atmospheres*, *126*, e2021JD035478. https://doi.org/10.1029/2021JD035478

Received 28 JUN 2021
Accepted 1 NOV 2021

Abstract Controls on the particle size distribution (PSD) of mineral dust emissions remain poorly understood. Under near-idealized conditions, dust PSDs can appear invariant with wind friction velocity. However, dryland vegetation attenuates surface friction velocities, and soil crusting reduces the supply of loose erodible material and increases surface resistance to abrasion. Under such conditions, variability in saltation bombardment efficiency and intensity could have a large effect on dust PSDs. We present dust emission measurements from vegetated, supply-limited aeolian systems that indicate the dependence of emission-flux PSD on wind friction velocity. We find the fine fraction (<5 μm) of dust particles increases with friction velocity. Results suggest models that assume wind-invariance of the emission-flux PSD may not be generalizable for crusted soils with vegetation. There is a need for dust models to represent variability in emission-flux PSDs for land management, air quality, and climate applications across vegetated and sediment supply-limited drylands.

Plain Language Summary The size of dust particles emitted into the air during wind erosion determines how soils are affected and how dust influences air quality and climate. However, much remains unknown about how wind speed, soil properties, and vegetation influence the size of emitted dust at different locations. Some studies suggest that when land is unvegetated and soils are loose, the size of emitted dust does not change with wind speed. We measured the size of dust emitted from vegetated landscapes with soils that are crusted and have changing amounts of loose erodible sediment. We found that wind speed has a strong effect on the size of emitted dust particles. Stronger winds produced finer dust at sites with weaker soil crusts and more loose erodible sediment. Predictive models need to consider the changing size of emitted dust particles in different environments in order to more accurately assess wind erosion and dust impacts.

1. Introduction

The particle size distribution (PSD) of mineral dust is an important determinant of dust effects on radiative forcing, cloud and ice nucleation, precipitation, and biogeochemical cycling (Shao, Wyrwoll, et al., 2011). Dust PSD also influences dust effects on ecosystems and surface hydrology (Field et al., 2010), infrastructure, and human health (Middleton, 2017). In dust source areas, the emission of different sized dust particles coarsens soil texture by selective removal of fine particles (Li et al., 2009), and reduces soil productivity through loss of nutrients and carbon (Webb et al., 2012). Dust PSD is a critical control of dust transport and deposition rates, which influence residence time in the atmosphere, transport distance, and the lifetime of interactions (Mahowald et al., 2014). Dust emission flux from a landscape is determined by the magnitude of the wind friction velocity, u_* (the square root of the surface shear stress divided by air density), and aerodynamic lift and saltation bombardment processes that emit fine particles into the air (Gillette, 1981). Understanding these controls on the PSD of emitted dust is therefore critical for predicting and assessing onsite and downwind impacts of mineral dust emission (Kok, 2011). However, uncertainty remains regarding the sensitivity of emission-flux PSDs to u_*, and whether the dependence changes under transport-limited conditions, where sediment entrainment is controlled by the wind force and other aerodynamic factors such as atmospheric boundary layer (ABL) stability, or supply-limited conditions under which sediment entrainment is controlled by the amount of loose erodible material (LEM) at the soil surface.

The current understanding of dust PSD dependence on u_* is largely based on measurements acquired under near-idealized conditions. Shao et al. (2020) identified that studies have described PSD of dust at source at height zero (emission-dust PSD), PSD of dust suspended in the air (airborne-dust PSD), and dust emission-flux PSD that is predicted by dust emission models. Conditions of previous studies include wind tunnel experiments (Alfaro et al., 1997; Gillette et al., 1974) and field measurements from bare agricultural fields or other largely unvegetated landscapes with the near-unlimited supply of LEM, and fetch sufficient for transport-limited equilibrium saltation (e.g., Fratini et al., 2007; Gillette et al., 1972; Gillies & Berkofsky, 2004; Huang et al., 2019; Shao, Ishizuka, et al., 2011; Sow et al., 2009; Zobeck & Van Pelt, 2006). Some measurements under near-idealized conditions indicate there is no statistically significant dependence of emission-flux PSD on u_* (Kok, 2011). This finding is supported by empirical studies (e.g., Creyssels et al., 2009; Martin & Kok, 2017) and theoretical models showing that mean saltator impact speed, which determines bombardment intensity, has little dependence on mean wind speed during equilibrium saltation (Durán et al., 2011; Kok et al., 2012). However, other measurements and modeling suggest emission-dust PSD and emission-flux PSD are sensitive to variability in u_* and ABL stability (Alfaro et al., 1997; Dupont et al., 2015; Khalfallah et al., 2020; Sow et al., 2009; Shao et al., 2020). Inconsistent measurement approaches among studies have inevitably compounded the difficulty of resolving how land surface and atmospheric conditions influence the emission-flux PSD.

Understanding how sensitive emission-flux PSD is to u_* is important for understanding wind erosion impacts and modeling dust cycle interactions with Earth systems (Shao, 2008). Current dust models reflect the different experimental findings described above. Most assume that emission-flux PSD is invariant with u_* (e.g., Albani et al., 2014; Kok, Mahowald, et al., 2014; LeGrand et al., 2019; Pope et al., 2016), which enables simplification of emission schemes and application to available soil texture datasets (e.g., Kok, Albani, et al., 2014). The alternative scheme of Shao (2004) relates dust emission flux for given particle size (d) to saltation bombardment intensity and aggregate disintegration, which depend on u_* and inter-particle cohesion. The scheme predicts that emission-flux PSD varies with u_* and the source soil PSD but relies on detailed soil particle size information for which global data are not currently available (Shao, 2004). The assumption of emission-flux PSD invariance with u_* in dust models is consistent with the use of saltation mass flux equations that assume saturated or equilibrium transport (Sherman, 2020). However, while this may be reasonable in some barren and very sparsely vegetated dust sources (<12% of Earth's land surface), near-idealized conditions for dust emission likely occur rarely in vegetated drylands and croplands that comprise significantly more (55%) of Earth's land surface (Friedl et al., 2010), are more densely populated, and dust impacts on soils, ecosystems, and communities are most strongly felt (Middleton et al., 2019). Understanding the nature and controls on emission-flux PSD in these environments is therefore critical for forecasting and mitigating dust impacts.

Conditions that could induce variability in emission-flux PSD with u_* include changes in availability and PSD of LEM that can be entrained by wind (Gillette & Chen, 2001; Klose et al., 2017), variability in cohesive properties of soil that influence surface deformation, and abrasion during saltation (Houser & Nickling, 2001; Rice et al., 1999; Shao, Ishizuka, et al., 2011), and variability in turbulent momentum fluxes from surface roughness and buoyancy in the ABL (Dupont et al., 2019; X. Li & Bo, 2019). These conditions are found in many drylands, including agricultural landscapes, where vegetation is present and soils contain sufficient silt and clay to promote sediment supply limitation through aggregation and crusting (Webb & Strong, 2011). Under such conditions, saltation and surface bombardment is more likely to be unsteady and spatially variable (Durán et al., 2011) as saltators speed up and slow down across the surface (Shao et al., 2020).

Here, we aim to establish whether dust emission-flux PSD has statistically significant variability with u_* over vegetated and sediment supply-limited dryland soils. We resolve the sensitivity of emission-flux PSD to u_* for 10 dust events measured across three sites in the Chihuahuan Desert, New Mexico, USA. As a step toward understanding the influence of environmental conditions on emission-flux PSD, we interpret variability of emission-flux PSD in the context of soil and vegetation characteristics including physical crusting and LEM that induce sediment supply-limitation, and vegetation that determines surface wind shear stress and the duration of saltation. Elucidating the dependence of emission-flux PSD on u_* for vegetated and sediment supply-limited landscapes are needed to inform the selection of parameterization schemes, and

Table 1
Characteristics of the Measured Dust Events, Including Surface (0–1 cm) Soil Texture, Mean and Range of Wind Friction Velocity (u_*), Percent Cover of Properties Controlling Site Potential to Emit Dust Particles, Including Loose Erodible Material (LEM; <2 mm), Physical Crust (PC), Aggregates (AG; >2 mm), Gravel (GR; >2 mm) and Foliar Cover of Vegetation and Detached Litter at the Soil Surface, and Mean and Standard Deviation (SD) of the Vertically-Integrated Horizontal Sediment Mass Flux Q

		Soil texture				Surface cover (%)						Wind direction (°)	Friction velocity (m s^{-1})		Q (g m^{-1} s^{-1})	
Site	Event	Sand (%)	Silt (%)	Clay (%)	Texture class	LEM	PC	AG	GR	Foliar cover	Total litter	Range	Mean	Range	Mean	SD
Site 3	2017/04/28	53.6	21.5	24.9	Sandy clay loam	9.2	88.5	2.0	0.3	1.0	0.2	213–236	0.36	0.26–0.45	0.002	0.0005
	2018/04/08					6.2	91.0	1.7	1.2	1.0	3.2	222–265	0.36	0.28–0.43	0.006	0.007
	2018/04/17					6.2	90.0	2.5	1.4	0.7	3.0	210–253	0.42	0.14–0.56	0.011	0.003
Site 4	2017/04/25	61.4	22.3	16.3	Sandy loam	88.7	6.0	1.3	3.8	16.3	5.3	244–268	0.73	0.53–0.87	1.131	0.814
	2017/04/27					85.8	8.3	0.8	4.8	15.7	5.5	213–254	0.62	0.47–0.73	0.296	0.149
	2017/05/25					85.7	8.7	0.2	5.0	17.7	6.3	225–264	0.46	0.34–0.69	0.170	0.150
	2018/03/18					50.0	42.2	0.2	6.5	12.8	11.2	219–269	0.66	0.45–0.85	0.550	0.235
Site 5	2017/05/16	67.1	21.9	11.0	Sandy loam	81.5	16.7	0.7	0.6	18.7	9.5	207–291	0.63	0.33–0.99	1.092	0.696
	2018/03/15					72.3	26.7	0.2	0.5	14.5	21.3	212–259	0.73	0.52–0.99	1.332	1.002
	2018/05/02					70.0	26.8	1.3	1.5	22.0	19.8	210–263	0.73	0.57–0.90	0.123	0.089

Note. Soil surface texture data were determined by laser particle size analysis as reported in Webb et al. (2016).

development of new models, to ensure realistic representation of the particle size characteristics of mineral dust emissions from drylands.

2. Methods

2.1. Data Collection

Measurements were collected during 10 dust emission events in March to May of 2017 and 2018 at three sites on the Jornada Experimental Range in south-central New Mexico, USA. The study sites were named Site 3 (playa), Site 4 (mixed bunchgrasses and forbs), and Site 5 (open shrubland), as described by Webb et al. (2016). Table 1 summarizes site characteristics for the dust events, measured using methods described below. Each site was enclosed in a 20 × 20 m fence to exclude livestock and vegetation within the fenced areas was clipped in March and April (early growing season) each year to avoid interference or obstruction of instrumentation for the duration of the study.

Atmospheric conditions were measured with centrally-located meteorological towers equipped with RM Young 3101 cup anemometers at heights of 0.7 m, 1.4, and 2.4 m above ground level, and one RM Young 3002 anemometer and wind vane at 4.8 m height. Temperature sensors (Campbell Scientific 107-L) were mounted in solar radiation shields at 2.0 and 4.0 m heights. Data were sampled at 1 Hz and were logged every 1 min on Campbell Scientific CR1000 data loggers.

Dust concentrations were measured using a pair of optical particle sizer (OPS) spectrometers (TSI model 3330) with omnidirectional sampler inlets (TSI model 8535) mounted on a mast at 1.25 and 2.5 m heights adjacent to the meteorological tower. The spectrometers were configured to measure count size distributions and reported concentrations for particles in 12 bins with diameters 0.3–0.5, 0.5–0.7, 0.7–1.0, 1.0–1.5, 1.5–2.0, 2.0–2.5, 2.5–3.0, 3.0–4.0, 4.0–5.0, 5.0–6.0, 6.0–8.0, 8.0–10.0 μm. Inlet aspiration efficiency tests by TSI show that at an inlet flow rate of 1.7 L min^{-1}, the mass concentration collection efficiency for PM_{10} varied from ~100% at 2.2 m s^{-1} to 80% at 6.3 m s^{-1}, suggesting some under-sampling of coarser particles may have occurred during dust emission episodes associated with stronger wind gusts (TSI Inc., 2012). The instruments were calibrated by TSI with Polystyrene Latex (PSL) spheres to the ISO 21505-01/04 standard prior to deployment in the field so that between-sampler performance was established as consistent under laboratory conditions. We converted particle number concentrations to mass concentrations assuming

sphericity and a dust particle density of 2,500 kg m^{-3}, consistent with Arizona test dust (ISO 12103–1, A1). The instruments were programmed to commence sampling between 09:30 a.m. and 11:30 a.m. local time, depending on forecast wind speeds, and sampled and logged at 1 Hz continuously for 8 hr. Horizontal sediment mass flux was measured using Modified Wilson and Cooke (MWAC) sediment samplers with inlet 2.34×10^{-4} m^2 (Webb et al., 2019). Five freely rotating masts, each with four MWAC samplers (0.1, 0.25, 0.5, and 0.85 m above ground level) were located surrounding the meteorological towers. Samplers were installed on the masts when the OPS spectrometers commenced measuring and were removed after 8 hr to provide the cumulative total horizontal sediment mass flux for each dust event.

Three parallel 50 m transects spaced 25 m apart were established and measured through the sites with the central transect passing through the center of the fenced areas. On the morning of each event, methods of Herrick et al. (2018) were used to measure vegetation height every 2 m, the size distribution of canopy gaps ≥ 5 cm (unvegetated spaces between plant canopies), and foliar cover of vegetation by species and soil surface properties including presence of LEM (<2 mm diameter), physical crust, broken crust (aggregates >2 mm), fine gravel (2–5 mm), and gravel (5–76 mm) every 0.25 m. Soil surface disturbance and vegetation removal, and the overall site vegetation structure that is important for momentum partitioning (Li et al., 2013; Okin, 2008), were captured by the transect observations. To support interpretation, qualitative observations were made of the timing of dust emission, for example, associated with the passage of turbulent eddies over the sites.

2.2. Data Analysis

Wind flow over the study sites experiences drags from vegetation, resulting in partitioning of wind momentum flux and reduction of the friction velocity at the soil surface (u_{s*}) that drives saltation and dust emission. Previous research at the sites demonstrated that estimates of the aerodynamic roughness length (z_0) and u_* had large variability due to changing wind direction over the heterogeneous roughness (Ziegler et al., 2020). To account for uncertainty in u_* due to the drag partition, we considered the influence of both u_* and u_{s*} on the emission-flux PSDs. Wind friction velocity (u_*) was estimated following the Prandtl-von Kármán logarithmic velocity profile law:

$$u_* = \frac{kU_z}{\ln\left(\frac{z}{z_0}\right)} \tag{1}$$

where U_z is the wind speed (m s^{-1}) at height z (m), u_* is the wind friction velocity (m s^{-1}) and k is von Kármán's constant (~0.4). Following Klose et al. (2019), wind speed data were resampled to 15 min running averages from which z_0 and u_* were obtained by linear regression:

$$U_z = m \cdot ln(z) + c, \tag{2}$$

where $u_* = mk$ and $z_0 = e^{-c/m}$. To ensure thermal neutrality for a logarithmic profile, we selected only periods with wind speeds at all heights >2 ms^{-1}, and fit of the vertical wind speed data to Equation 2 as defined by the correlation coefficient $r^2 > 0.97$, and $\Delta T_{2m-4m} < 0.5°C$.

We estimated u_{s*} using the Okin (2008) drag partition scheme with 15 min running mean of the 1 min wind speed (U_z) measured at 4.8 m above ground level, and detailed measurements of vegetation height and canopy gap size distribution from the transects, following:

$$\left(u_{s*} / u_*\right) = \left(u_{s*} / u_*\right)_{x=0} + \left[1 - \left(u_{s*} / u_*\right)_{x=0}\right]\left[1 + Exp\left(xc_1 / h\right)\right], \tag{3}$$

where $(u_{s*}/u_*)_{x=0}$ is the wind friction velocity reduction immediately leeward of a roughness element, x is the length of bare gaps between plants, h is the mean plant height, and c_1 defines the rate of wind recovery at a given x/h. To account for uncertainty in the parameterization of the drag partition, we estimated median predictions of u_{s*} for each dust event using parameter ranges of $-4 < \log[z_0] < -1$, $0 < (u_{s*}/u_*)_{x=0} < 0.5$, and $2 < c_1 < 8$ following Okin (2008) and Li et al. (2013).

We calculated streamwise saltation fluxes, Q (g m^{-1}s^{-1}) for each MWAC mast using nonlinear least squares regression to fit exponential functions to the data. We then integrated from 0 to 1.0 m height and divided by the sampling period to obtain:

$$Q = \int_0^1 q(z)dz, \tag{4}$$

where $q(z)$ is the sediment mass collected per unit inlet area (m^{-2}) per sampling period (8 hr) at heights z (m).

We used the gradient method of Gillette et al. (1972) to calculate the dust emission flux F_d (μg m^{-2} s^{-1}) for 15 min running means of the 1 min dust concentrations c at different heights for each particle size bin (d) following:

$$F_d = -K_p \frac{c_2 - c_1}{z_2 - z_1}, \tag{5}$$

where c_2 and c_1 are dust concentrations and z_2 and z_1 are heights of OPS spectrometers mounted at 2.5 m (OPS 2) and 1.25 m (OPS 1) respectively. The eddy diffusivity K_p (m^{-2} s^{-1}) of the dust particles was calculated as:

$$K_p = ku_*\bar{z}, \tag{6}$$

where k is the von Kármán constant (~0.4) and $\bar{z}$ is the mean of heights z_2 and z_1 (Csanady, 1963; Gillette et al., 1972). As the OPS spectrometer inlets were mounted above the measured maximum vegetation heights at Site 3 (0.74 m), Site 4 (0.44 m), and Site 5 (1.06 m), we calculated K_p as a function of u_*, representative of local eddies diffusing dust above the vegetation, for the particle size bins measured by the spectrometers. To ensure F_d represent the local emission flux for different particle sizes, and remove airborne dust influenced by advection, we filtered the data to retain only periods with a positive vertical dust flux and excluded measurements from periods when the PM10 concentration did not exceed two standard deviations of a 15 min running mean of the PM10 concentration at 2.5 m. The remaining dust concentrations and F_d were qualitatively cross-checked for consistency with our field observations of onsite dust emission to provide reassurance that measured positive emission fluxes occurred when we visually saw dust emission occurring. We then calculated the emission-flux PSD for each particle size bin at d_j with bin size Δd_j as:

$$p(d_j)\Delta d_j = F_j / \sum F_j \tag{7}$$

where F_j is the dust flux for particle size bin j (Shao et al., 2020). To test the sensitivity of emission-flux PSD to friction velocity, we ran a non-parametric Kruskal-Wallis analysis of variance (ANOVA; Kruskal & Wallis, 1952) of emission-flux PSD by u_* and u_{s*} categories of 0–0.1, 0.1–0.2, 0.2–0.3, 0.3–0.4, 0.4–0.5, 0.5–0.6, 0.6–0.7, 0.7–0.8, 0.8–0.9 and 0.9–1.0 m s^{-1} respectively for each dust event. Including u_* and u_{s*} bins <0.2 ms^{-1} was necessary to represent the range of mean boundary-layer conditions under which dust emission occurred at the 15 min time scale, which incorporates the instantaneous scaling of dust emission fluxes with turbulence and surface shear stress fluctuations (Shao et al., 2020). Including u_{s*} enabled us to assess the dependency of the emission-flux PSDs on wind friction velocity at the soil surface driving saltation and dust emission. The Kruskal-Wallis ANOVA tests the hypothesis that different samples being compared from two or more groups (i.e., $p(d_j)\Delta d_j$ for each u_* and u_{s*} bin) are from the same distribution, but does not assume the residuals are normally distributed (Kruskal & Wallis, 1952). Data from the 0.3–0.5 μm and 1.5–2.0 μm particle size bins sporadically reported spurious values during the events and so were removed from the analysis. When significant differences ($p < 0.05$) among $p(d_j)\Delta d_j$ across u_* and u_{s*} categories were detected by the Kruskal-Wallis test, we computed post-hoc comparisons of mean ranks of all pairs of particle size bin, u_* and u_{s*} categories using Dunn's test with Bonferroni adjustment. The analysis revealed whether a change in u_* or u_{s*} during each dust event produced a significant change in emission-flux PSD between specific pairs of particle size bins.

3. Results

Measured emission-flux PSDs had statistically significant ($p < 0.05$) dependence on wind friction velocity (u_*) for some dust events at each of the three study sites (Figure 1 and Table 2). The range of u_* categories over which dust emission occurred at vegetated Sites 4 and 5 was greater than for playa Site 3, which was largely free of vegetation in the dominant wind directions for the events (210°–265°). Figure 1 shows that during events with larger u_*, there was a clear but not systematic increase in the proportion of fine particles (1–5 μm) comprising the emission-flux PSDs. Significant increases in the submicron dust fraction were also measured for some events. Fewer significant changes were detected in the proportion of 5–10 μm dust particles across the 10 events, although our results show there was a pattern of a proportional decrease in coarser particles that was consistent with the increase in the finer fraction of the PSDs. Pairwise comparisons of the emission-flux PSDs among u_* categories using Dunn's test showed that there was variability in the number of PSDs that were significantly different within the measured dust events, but that was not always related to the range of measured u_* and the number of u_* categories (Table 2). That is to say that, where statistically significant differences between emission-flux PSDs were detected by the Kruskal-Wallis ANOVA, significant differences were not necessarily detected between PSDs for every u_* category.

We found a strong dependence of emission-flux PSD on surface wind friction velocity (u_{s*}) resulting from the vegetation-induced drag partition (Figure 2 and Table 2). Eight of the 10 events showed a statistically significant dependence of emission-flux PSD on u_{s*} for three or more of the 10 particle size bins. While the eddy diffusivity between the OPS spectrometers is described by u_*, generation of the dust emission flux is dependent on the instantaneous magnitude of wind shear stress at the soil surface driving saltation and so the dependency between emission-flux PSD and small u_{s*} is not surprising. At Site 3, the Okin (2008) drag partition predicted u_{s*} generally consistent with u_* measured for the playa surface. There was a substantial reduction in u_{s*} relative to u_* at vegetated Sites 4 and 5, with periodic overestimation of u_{s*} at Site 3 due to uncertainty represented in the model parameterization of z_0 (Supporting Information S1). This uncertainty in the estimated u_{s*} may have influenced the dependence of emission-flux PSD on u_{s*}, resulting in differences in the Kruskal-Wallis test results between u_* and u_{s*} at Site 3 (Table 2). However, overall good consistency between measured u_* and estimated u_{s*} at Site 3, and large uncertainty in measured u_* at Sites 4 and 5 due to the heterogeneous vegetation height and spatial distribution (Ziegler et al., 2020), provide confidence that estimated u_{s*} is at least as robust as the measurements for assessing the emission-flux PSD dependence. Pairwise comparisons of the emission-flux PSDs among u_{s*} categories using Dunn's test showed fewer pairs of PSDs were significantly different than among u_* categories–largely because there were fewer u_{s*} categories due to the drag partition reducing the mean surface momentum flux.

Dust events at Site 4 on April 25, 2017 and Site 5 on May 16, 2017 showed the strongest dependence of emission-flux PSD on u_{s*}. Increasing u_{s*} produced emission flux PSDs with a larger proportion of fine dust particles (<5 μm) relative to the 5–10 μm fraction. The event at Site 4 had the largest mean u_*, the largest cover of LEM, the smallest percent cover of physical crust, and the largest saltation flux of all events measured at that site (Table 1). The Site 5 event had the second-largest measured saltation flux out of five events at that site, with the largest percent cover of LEM and the smallest percent crust cover of the events at that site. Emission-flux PSDs at Site 3 on April 8, 2018, and April 17, 2018, were less dependent on u_{s*} than the event on April 28, 2017, although the April 17, 2018 event showed statistically significant dependence on u_* for seven of the 10 particle size bins. The events at Site 3 had the largest percent cover of a physical soil crust, smallest percent cover of LEM, and smallest saltation fluxes of the three study sites.

4. Discussion and Conclusions

Our results show there is a clear dependence of emission-flux PSD on wind friction velocity for vegetated and sediment supply-limited aeolian systems. Consistent with Shao et al. (2020), we found statistically significant variability in emission-flux PSD and a tendency for the fine fraction (<5 μm) of dust particles to proportionally increase with increasing friction velocities and saltation fluxes. This finding contradicts the main conclusion of Kok (2011), that the size distribution of naturally emitted dust aerosols is invariant with wind speed at emission. However, it is consistent with Kok's (2011) observation that wind speed independence of emission-flux PSDs may be restricted to transport-limited saltation conditions. Our results

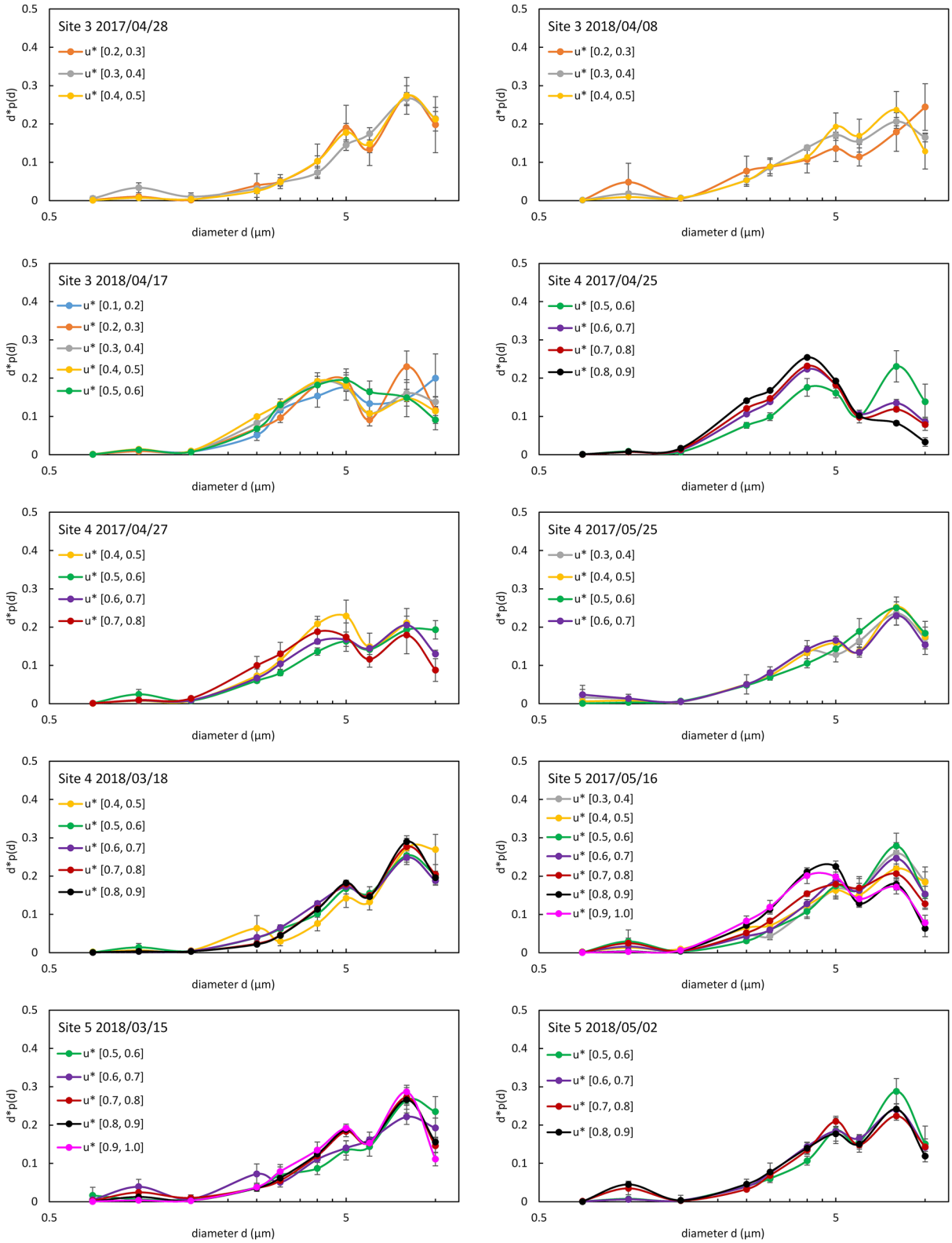

Figure 1. Emitted-dust particle size distribution with standard error for different wind friction velocity (u_*) categories for the 10 dust events.

Table 2
Summary of Kruskal-Wallis Analysis of Variance by Ranks, Showing Sample Size (N) and p Values ($p < 0.05$ Bold) for Differences in Emission-Flux Particle Size Density for Each Friction Velocity (u_*) and Surface Friction Velocity (u_{s*}) for Each Particle Size Bin

				Dust particle size bin (μm)									
Site	Event	*N*	Friction velocity	0.5–0.7	0.7–1.0	1.0–1.5	2.0–2.5	2.5–3.0	3.0–4.0	4.0–5.0	5.0–6.0	6.0–8.0	8.0–10
Site 3	2017/04/28	291	u_*	0.7961	0.4425	0.2771	0.0321	0.0620	**0.0080**[1]	**0.0019**[1]	0.2406	0.8271	0.2244
			u_{s*}	0.6144	0.3343	0.1633	**0.0228**	**0.0172**	**<0.000**[3]	**0.0002**[2]	**0.0064**[1]	0.5404	0.3346
	2018/04/08	279	u_*	0.9020	0.1772	0.6346	0.4047	0.6831	**0.0461**	0.2892	0.6704	0.7194	0.4651
			u_{s*}	0.5901	**0.0422**	0.6078	0.3886	0.8878	0.1616	0.2943	0.5861	0.5616	0.2799
	2018/04/17	322	u_*	**<0.000**[3]	**0.0171**[1]	**0.0118**[2]	**0.0009**[1]	**0.0095**[1]	0.1762	0.7324	0.6972	**0.0016**[2]	**0.0001**[1]
			u_{s*}	0.2359	0.8520	0.9131	**0.0282**[1]	0.2924	0.7090	0.7581	0.8051	0.2039	**0.0456**
Site 4	2017/04/25	375	u_*	**<0.000**[4]	**0.0048**[2]	**<0.000**[6]	**<0.000**[6]	**<0.000**[5]	**<0.000**[4]	0.2040	0.8601	**<0.000**[5]	**<0.000**[4]
			u_{s*}	**<0.000**[1]	**<0.000**[1]	**<0.000**[1]	**<0.000**[1]	**<0.000**[1]	**<0.000**[1]	0.3775	**<0.000**[1]	**<0.000**[1]	**<0.000**[1]
	2017/04/27	423	u_*	**0.0057**[1]	0.7783	**<0.000**[2]	**0.0007**[2]	**0.0064**[1]	**0.0024**[1]	0.3183	0.2768	0.6616	0.0660
			u_{s*}	**<0.000**[2]	0.7460	**<0.000**[3]	**<0.000**[3]	**<0.000**[2]	**<0.000**[2]	0.2243	**0.0053**[2]	**0.0311**[1]	0.9507
	2017/05/25	425	u_*	0.3958	**<0.000**[4]	**0.0001**[3]	**<0.000**[3]	0.1357	0.1401	**0.0219**[1]	0.1601	0.9099	0.5330
			u_{s*}	0.5449	**0.0006**[1]	**<0.000**[1]	**<0.000**[1]	**<0.000**[1]	**<0.000**[1]	**<0.000**[1]	0.6928	0.6278	0.3448
	2018/03/18	335	u_*	**<0.000**[3]	0.7113	**<0.000**[5]	0.0528	**<0.000**[4]	**<0.000**[4]	0.1771	0.7726	**0.0408**	0.1207
			u_{s*}	**0.0281**	0.3510	**<0.000**[2]	**0.0172**[1]	**<0.000**[1]	**<0.000**[1]	**0.0048**[1]	0.6087	0.3764	0.0857
Site 5	2017/05/16	410	u_*	**0.0065**[2]	**<0.000**[7]	**<0.000**[11]	**<0.000**[10]	**<0.000**[11]	**<0.000**[11]	0.0574	0.7306	**0.0300**	**0.0012**[2]
			u_{s*}	0.3272	**<0.000**[1]	**<0.000**[4]	**<0.000**[3]	**<0.000**[4]	**<0.000**[3]	**0.0046**[1]	0.3261	**0.0236**	**0.0028**[1]
	2018/03/15	426	u_*	**0.0321**[1]	0.4439	0.2229	**0.0205**	**0.0003**[1]	**<0.000**[5]	**<0.000**[6]	0.5314	0.3799	0.1951
			u_{s*}	0.8081	0.6209	**0.0034**[1]	**<0.0000**[1]	**<0.0000**[1]	**<0.0000**[1]	**0.0044**[1]	0.3206	0.8920	0.5483
	2018/05/02	241	u_*	**0.0090**[1]	**0.0139**[1]	0.0613	**0.0126**[1]	0.5974	0.3978	0.3854	0.4125	0.5221	0.8163
			u_{s*}	0.7719	**0.0261**	**0.0446**	**0.0389**[1]	0.0633	**0.0180**	0.1819	**0.0430**	0.0793	**0.0479**

Note. Superscript numbers indicate the number of pairs of u* or us* groups that showed significant differences in post-hoc comparisons of mean ranks of emission-flux probabilities using Dunn's test with Bonferroni adjustment.

corroborate previous studies that suggest emission-flux PSDs can show statistically significant variability under different environmental conditions—from unvegetated fields to desert landscapes, and across a range of wind speed and ABL stability conditions (e.g., Khalfallah et al., 2020; Shao et al., 2020). Possible mechanisms driving variability in emission-flux PSDs that are influenced by soil crusting and vegetation include varying saltation bombardment intensities with fluctuating wind speeds (Dupont et al., 2015), varying availability of different size LEM under sediment supply-limited conditions (Houser & Nickling, 2001; Rice et al., 1996), and varying saltator impact speeds if equilibrium saltation is not established (Alfaro et al., 1998). ABL stability may also be important for variability in emission-flux PSDs, with increased turbulence under unstable conditions producing larger variability in saltation bombardment intensity than under stable conditions (Shao et al., 2020), and instability potentially increasing the efficiency of transfer of dust particles away from the soil surface (Khalfallah et al., 2020). We interpret the effect of vegetation at the study sites as influencing near-surface turbulence, surface shear stress, and saltation interception by plants, which according to Wolfe and Nickling (1993) and Poggi et al. (2004), can promote unsteady surface shear stress and intermittent saltation. Consistent with observations of Stout and Zobeck (1996) for aerodynamically rough field surfaces, such conditions would reduce the likelihood of saltation reaching transport capacity and so enable saltator particle velocities to vary and increase with increasing wind speed (Durán et al., 2011), potentially producing more surface abrasion (Rice et al., 1999) and change in emission-flux PSDs. While our interpretation of the mechanisms explaining variability in the emission-flux PSD and increase in fine particle emissions with increasing friction velocity is supported by the above-cited studies, it should be acknowledged that, in the absence of more detailed meteorological observations and direct measurements of dynamic surface properties and saltator speeds, such interpretation does remain

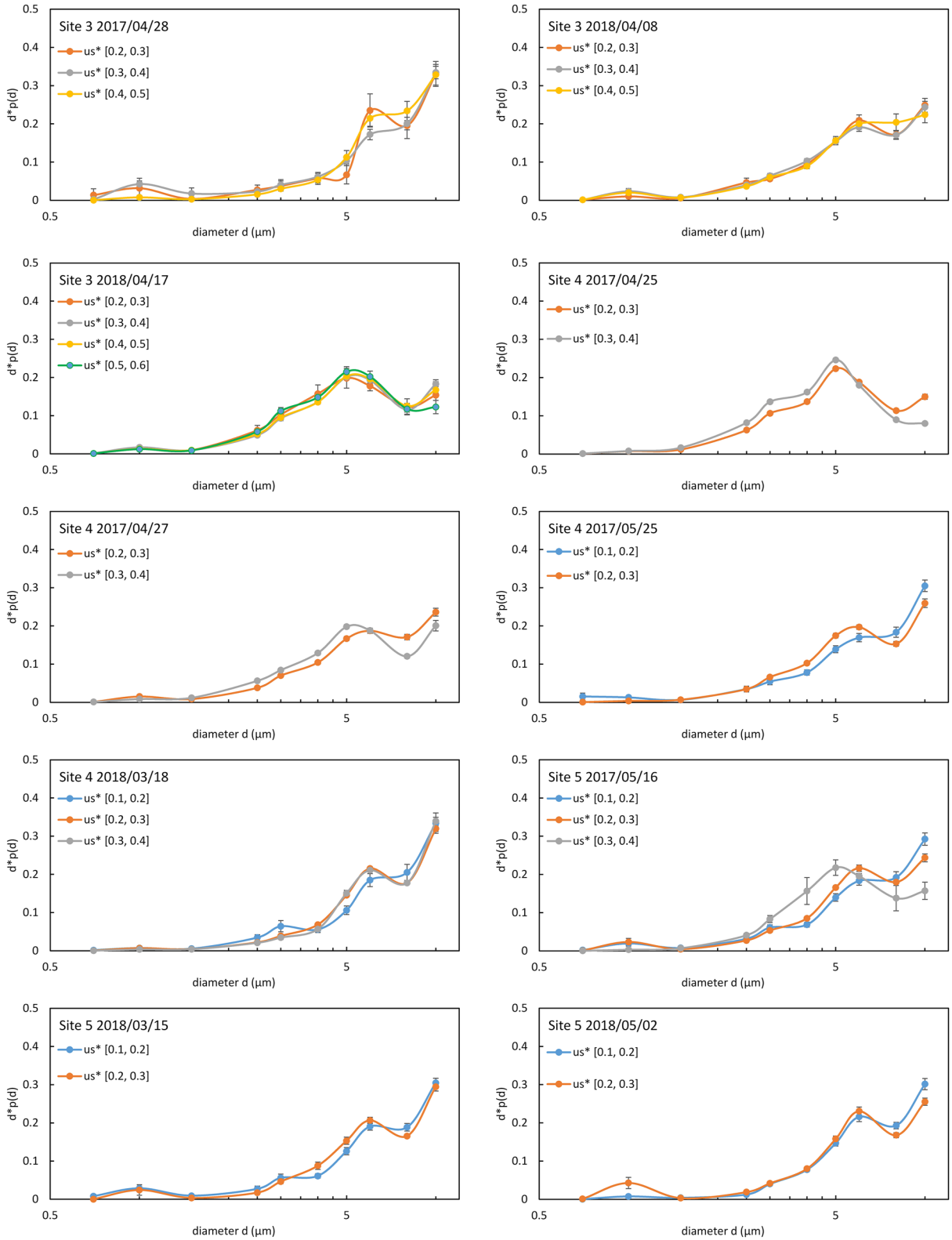

Figure 2. Emitted-dust particle size distribution with standard error for different surface wind friction velocity (u_{s*}) categories for the 10 dust events.

uncertain. Future field and wind tunnel research that is able to simultaneously measure around vegetation the saltation flux, saltator particle sizes, and particle speeds, and changing crust cover and crust resistance to abrasion, alongside emission-flux PSD, may be able to resolve the mechanisms more directly. A requisite step in understanding the effects of these different controls on variability in emission-flux PSDs will be quantitatively determining how much soil crusting (e.g., percent cover) is needed to induce sediment supply-limited saltation and when subsequent changes in emission-flux PSD are due to dust particle enrichment or depletion.

Interestingly, emission-flux PSD was not dependent on wind friction velocity for all our measured events and was largely invariant with measured u_* during two events on the heavily crusted playa Site 3. Crust hardness measurements to rupture reported by Webb et al. (2016) show the playa surface was likely more resistant to abrasion (penetrometer hardness 1.87 $\pm$ 0.99 kg cm^{-2}) than the weakly-crusted soils at Site 4 (0.54 $\pm$ 0.02 kg cm^{-2}) and Site 5 (0.50 $\pm$ 0.01 kg cm^{-2}). These measurements remained representative of the conditions at the sites during the measured events as we observed little crust disturbance under foot on the playa, while crusts at Sites 4 and 5 were easily broken and were striated from abrasion during the events. The playa Site 3 also had a substantially smaller percent cover (6.2%–9.2%) of LEM than Sites 4 and 5 (Table 1) that likely further limited dust emission potential by reducing the saltation flux (Zobeck, 1991). Webb et al. (2016) showed that differences in physical crusting had little effect on the saltation threshold among the sites. It, therefore, appears that sediment supply limitation may not be described well by differences in saltation threshold, but is dependent on the size and availability of LEM. Our results indicate that dust emission from the supply-limited playa site was most likely controlled by a combination of the mass flux of available saltators (LEM), and crust resistance to abrasion (Houser & Nickling, 2001). At low friction velocities, very small saltation fluxes over the hard crusted playa soil produced dust emission fluxes with largely wind-invariant PSDs. Under higher friction velocities that produced a larger saltation flux, the emission-flux PSD showed dependence on u_*. Notably, while there was weak-to-no dependence of emission-flux of 5 μm dust on u_* or u_{s*} for the measured events at Site 3, some variability in the emission-flux PSD among events was apparent (Figures 1 and 2). However, a clear driver of this variability among events was not apparent from our soil surface measurements and our interpretation of the controls is based on understanding from previous research at the site. More detailed measurements of the soil crust and LEM PSDs would likely be needed to address mechanistically why the measured emission-flux PSDs varied across different particle sizes among u_* categories and dust events. Further research is needed at this site to resolve the relative effects of saltation mass flux and crust abrasion resistance on the variability of emission-flux PSDs.

Our finding of statistically significant variability in emission-flux PSDs calls into question the applicability of dust models that assume transport-limiting conditions and wind invariance of the emission-flux PSD to typical dryland landscapes (e.g., Kok, Mahowald, et al., 2014; LeGrand et al., 2019; Pope et al., 2016). Transport-limiting conditions for saltation and dust emission may occur on sandy soils and within barren lands of some major dust source regions (e.g., North Africa, Middle East, and Asia). However, supply-limiting conditions caused by soil crusting and vegetation likely occur across most semi-arid and arid drylands where wind erosion and dust effects on soils, agroecosystems, and communities are recognized as being important (Middleton, 2017). On vegetated and crusted soils under supply-limiting conditions, steady-state saltation may not be reached (e.g., Stout, 1990; Stout & Zobeck, 1996), the speed of saltating particles changes with wind speed (Durán et al., 2011), and abrasion efficiencies and intensities may vary among dust events (Rice et al., 1999)—potentially causing variability in emission-flux PSDs across space and through time. If emission-flux PSDs vary as our results suggest, then models that explicitly represent the dependence of the emission-flux PSD on wind friction velocity and soil surface properties (e.g., Alfaro & Gomes, 2001; Shao, 2004) should perhaps more accurately predict emitted dust particle size characteristics than those that prescribe a fixed emission-flux PSD. Pragmatically, simplified dust models remain useful given the ease of application to available soil texture datasets. However, our results indicate a clear need for dust models to represent variability in emission-flux PSD to be useful for land management, air quality, and climate applications in vegetated and sediment supply-limited drylands.

Data Availability Statement

Data from this study can be accessed via Zenodo at doi:10.5281/zenodo.4697972.

Acknowledgments
Funding support for this research was provided by the U.S. Army Engineer Research and Development Center (ERDC) Basic Research Program "Resolving the Size Distribution of Mineral Dust" (FWIC: 2469K1/FAN: U4357455) sponsored by the Assistant Secretary of the Army for Acquisition, Logistics, and Technology (ASA-ALT), and USDA Natural Resources Conservation Service (67-3A75-17-469). We thank Samantha Cook, Stacey Doherty, Bruce Elder, Mike Morgan and Ashley Mossell for assistance collecting data. This research was a contribution to the Long Term Agroecosystem Research (LTAR) network supported by the U.S. Department of Agriculture (USDA). Permission to publish was granted by Director, ERDC Cold Regions Research and Engineering Laboratory. Any use of trade, product, or firm names is for descriptive purposes only and does not imply endorsement by the U.S. Government. The USDA is an equal opportunity provider and employer.

References

Albani, S., Mahowald, N. M., Perry, A. T., Scanza, R. A., Zender, C. S., Heavens, N. G., et al. (2014). Improved dust representation in the Community Atmosphere Model. *Journal of Advances in Modeling Earth Systems*, *6*, 541–570. https://doi.org/10.1002/2013MS000279

Alfaro, S. C., Gaudichet, A., Gomes, L., & Maille, M. (1997). Modeling the size distribution of a soil aerosol produced by sandblasting. *Journal of Geophysical Research*, *102*, 11239–11249. https://doi.org/10.1029/97jd00403

Alfaro, S. C., Gaudichet, A., Gomes, L., & Maille, M. (1998). Mineral aerosol production by wind erosionL aerosol particle sizes and binding energies. *Geophysical Research Letters*, *25*, 991–994. https://doi.org/10.1029/98gl00502

Alfaro, S. C., & Gomes, L. (2001). Modeling mineral aerosol production by wind erosion: Emission intensities and aerosol size distributions in source areas. *Journal of Geophysical Research*, *106*(D16), 18075–18084. https://doi.org/10.1029/2000jd900339

Creyssels, M., Dupont, P., Ould El Moctar, A., Valance, A., Cantat, I., Jenkins, J. T., et al. (2009). Saltating particles in a turbulent boundary layer: Experiment and theory. *Journal of Fluid Mechanics*, *625*, 47–74. https://doi.org/10.1017/s0022112008005491

Csanady, G. T. (1963). Turbulent diffusion of heavy particles in the atmosphere. *Journal of Atmospheric Science*, *20*, 201–208. https://doi.org/10.1175/1520-0469(1963)020<0201:tdohpi>2.0.co;2

Dupont, S., Alfaro, S. C., Bergametti, G., & Marticorena, B. (2015). Near-surface dust flux enrichment in small particles during erosion events. *Geophysical Research Letters*, *42*, 1992–2000. https://doi.org/10.1002/2015gl063116

Dupont, S., Rajot, J. L., Labiadh, M., Bergametti, G., Lamaud, E., Irvine, M. R., et al. (2019). Dissimilarity between dust, heat, and momentum turbulent transports during aeolian soil erosion. *Journal of Geophysical Research: Atmospheres*, *124*, 1064–1089. https://doi.org/10.1029/2018jd029048

Durán, O., Claudin, P., & Andreotti, B. (2011). On aeolian transport: Grain-scale interactions, dynamical mechanisms and scaling laws. *Aeolian Research*, *3*, 243–270. https://doi.org/10.1016/j.aeolia.2011.07.006

Field, J. P., Belnap, J., Breshears, D. D., Neff, J. C., Okin, G. S., Whicker, J. J., et al. (2010). The ecology of dust. *Frontiers in Ecology*, *8*(8), 423–430. https://doi.org/10.1890/090050

Fratini, G., Ciccioli, P., Febo, A., Forgione, A., & Valentini, R. (2007). Size-segregated fluxes of mineral dust from a desert area of northern China by eddy covariance. *Atmospheric Chemistry and Physics*, *7*, 2839–2854. https://doi.org/10.5194/acp-7-2839-2007

Friedl, M. A., Sulla-Menashe, D., Tan, B., Schneider, A., Ramankutty, N., et al. (2010). *MODIS Collection 5 global land cover: Algorithm refinements and characterization of new datasets, 2001-2012, Collection 5.1 IGBP Land Cover*. Boston UniversityUSARep.

Gillette, D. A. (1981). *Production of dust that may be carried great distances* (Vol. *186*, pp. 11–26). Geological Society of America. https://doi.org/10.1130/SPE186-p11

Gillette, D. A., Blifford, I. H., & Fryrear, D. W. (1974). Influence of wind velocity on size distributions of aerosols generated by wind erosion of soils. *Journal of Geophysical Research*, *79*, 4068–4075. https://doi.org/10.1029/jc079i027p04068

Gillette, D. A., Blifford, I. H., & Spencer, C. R. (1972). Measurements of aerosol size distributions and vertical fluxes of aerosols on land subject to wind erosion. *Journal of Applied Meteorology*, *11*, 977–987. https://doi.org/10.1175/1520-0450(1972)011<0977:moasda>2.0.co;2

Gillette, D. A., & Chen, W. (2001). Particle production and aeolian transport from a "supply-limited" source area in the Chihuahuan desert, New Mexico, United States. *Journal of Geophysical Research*, *106*(D6), 5267–5278. https://doi.org/10.1029/2000jd900674

Gillies, J. A., & Berkofsky, L. (2004). Eolian suspension above the saltation layer, the concentration profile. *Journal of Sedimentary Research*, *74*, 176–183. https://doi.org/10.1306/091303740176

Herrick, J. E., Van Zee, J. W., McCord, S. E., Courtright, E. M., Karl, J. W., & Burkett, L. M. (2018). Monitoring manual for grassland, shrubland, and savanna ecosystems. In *Core methods* (Vol. *1*, 2nd ed.), USDA-ARS Jornada Experimental Range.

Houser, C. A., & Nickling, W. G. (2001). The factors influencing the abrasion efficiency of saltating grains on a clay-crusted playa. *Earth Surface Processes and Landforms*, *26*, 491–505. https://doi.org/10.1002/esp.193

Huang, Y., Kok, J. F., Martin, R. L., Swet, N., Katra, I., Gill, T. E., et al. (2019). Fine dust emissions from active sands at coastal Oceano Dunes, California. *Atmospheric Chemistry and Physics*, *19*, 2947–2964. https://doi.org/10.5194/acp-19-2947-2019

Khalfallah, B., Bouet, C., Labiadh, M., Alfaro, S., Bergametti, G., Marticorena, B., et al. (2020). Influence of atmospheric stability on the size-distribution of the vertical dust flux measured in eroding conditions over a flat bare sandy field. *Journal of Geophysical Research: Atmospheres*, *125*, e2019JD031185. https://doi.org/10.1029/2019jd031185

Klose, M., Gill, T. E., Etyemezian, V., Nikolich, G., Ghodsi Zadeh, Z., Webb, N. P., & Van Pelt, R. S. (2019). Dust emission from crusted surfaces: Insights from field measurements and modelling. *Aeolian Research*, *40*, 1–14. https://doi.org/10.1016/j.aeolia.2019.05.001

Klose, M., Gill, T. E., Webb, N. P., & Van Zee, J. W. (2017). Field sampling of loose erodible material: A new system to consider the full particle-size spectrum. *Aeolian Research*, *28*, 83–90. https://doi.org/10.1016/j.aeolia.2017.08.003

Kok, J. F. (2011). Does the size distribution of mineral dust aerosols depend on the wind speed at emission? *Atmospheric Chemistry and Physics*, *11*, 10149–10156. https://doi.org/10.5194/acp-11-10149-2011

Kok, J. F., Albani, S., Mahowald, N. M., & Ward, D. S. (2014). An improved dust emission model - Part 2: Evaluation in the Community Earth System Model, with implications for the use of dust source functions. *Atmospheric Chemistry and Physics*, *14*, 13043–13061. https://doi.org/10.5194/acp-14-13043-2014

Kok, J. F., Mahowald, N. M., Fratini, G., Gillies, J. A., Ishizuka, M., Leys, J. F., et al. (2014). An improved dust emission model - Part 1: Model description and comparison against measurements. *Atmospheric Chemistry and Physics*, *14*, 13023–13041. https://doi.org/10.5194/acp-14-13023-2014

Kok, J. F., Parteli, E. J. R., Michaels, T. I., & Karam, D. B. (2012). The physics of wind-blown sand and dust. *Reports on Progress in Physics*, *75*, 106901. https://doi.org/10.1088/0034-4885/75/10/106901

Kruskal, W. H., & Wallis, W. A. (1952). Use of ranks in one-criterion variance analysis. *Journal of the American Statistical Association*, *47*, 583–621. https://doi.org/10.1080/01621459.1952.10483441

LeGrand, S. L., Polashenski, C., Letcher, T. W., Creighton, G. A., Peckham, S. E., & Cetola, J. D. (2019). The AFWA Dust Emission Scheme for the GOCART Aerosol Model in WRF-Chem v3.8.1. *Geoscientific Model Development*, *12*, 131–166. https://doi.org/10.5194/gmd-12-131-2019

Li, J., Okin, G. S., & Epstein, H. E. (2009). Effects of enhanced wind erosion on surface soil texture and characteristics of windblown sediments. *Journal of Geophysical Research*, *114*, G02003. https://doi.org/10.1029/2008jg000903

Li, J., Okin, G. S., Herrick, J. E., Belnap, J., Munson, S. M., Miller, M. E., & Draut, A. E. (2013). Evaluation of a new model of aeolian transport in the presence of vegetation. *Journal of Geophysical Research*, *118*, 1–306. https://doi.org/10.1002/jgrf.20040

Li, X., & Bo, T. (2019). Statistics and spectra of turbulence under different roughness in the near-neutral atmospheric surface layer. *Earth Surface Processes and Landforms*, *44*, 1460–1470. https://doi.org/10.1002/esp.4588

Mahowald, N., Albani, S., Kok, J. F., Engelstaeder, S., Scanza, R., Ward, D. S., & Flanner, M. G. (2014). The size distribution of desert dust aerosols and its impact on the Earth system. *Aeolian Research*, *15*, 53–71. https://doi.org/10.1016/j.aeolia.2013.09.002
Martin, R. L., & Kok, J. F. (2017). Wind-invariant saltation heights imply linear scaling of aeolian saltation flux with shear stress. *Science Advances*, *3*, e1602569. https://doi.org/10.1126/sciadv.1602569
Middleton, N. J. (2017). Desert dust hazards: A global review. *Aeolian Research*, *24*, 53–63. https://doi.org/10.1016/j.aeolia.2016.12.001
Middleton, N. J., Tozer, P., & Tozer, B. (2019). Sand and dust storms: Underrated natural hazards. *Disasters*, *43*, 390–409. https://doi.org/10.1111/disa.12320
Okin, G. S. (2008). A new model of wind erosion in the presence of vegetation. *Journal of Geophysical Research*, *113*, F02S10. https://doi.org/10.1029/2007JF000758
Poggi, D., Porporato, A., Ridolfi, L., Albertson, J. D., & Katul, G. G. (2004). The effect of vegetation density on canopy sub-layer turbulence. *Boundary-Layer Meteorology*, *111*, 565–587. https://doi.org/10.1023/b:boun.0000016576.05621.73
Pope, R. J., Marsham, J. H., Knippertz, P., Brooks, M. E., & Roberts, A. J. (2016). Identifying errors in dust models from data assimilation. *Geophysical Research Letters*, *43*, 9270–9279. https://doi.org/10.1002/2016gl070621
Rice, M. A., McEwan, I. K., & Mullins, C. E. (1999). A conceptual model of wind erosion of soil surfaces by saltating particles. *Earth Surface Processes and Landforms*, *24*, 383–392. https://doi.org/10.1002/(sici)1096-9837(199905)24:5<383::aid-esp995>3.0.co;2-k
Rice, M. A., Willetts, B. B., & McKewan, I. K. (1996). Wind erosion of crusted soil sediments. *Earth Surface Processes and Landforms*, *21*(1), 279–293. https://doi.org/10.1002/(sici)1096-9837(199603)21:3<279::aid-esp633>3.0.co;2-a
Shao, Y. (2004). Simplification of a dust emission scheme and comparison with data. *Journal of Geophysical Research*, *109*, D10202. https://doi.org/10.1029/2003JD004372
Shao, Y. (2008). *Physics and modelling of wind erosion* (p. 393). Kluwer Academic Publishers.
Shao, Y., Ishizuka, M., Mikami, M., & Leys, J. F. (2011). Parameterisation of size-resolved dust emission and validation with measurements. *Journal of Geophysical Research*, *116*, D08203. https://doi.org/10.1029/2010JD014527
Shao, Y., Wyrwoll, K.-H., Chappell, A., Huang, J., Lin, Z., McTainsh, G. H., et al. (2011). Dust cycle: An emerging core theme in Earth system science. *Aeolian Research*, *2*, 181–204. https://doi.org/10.1016/j.aeolia.2011.02.001
Shao, Y., Zhang, J., Ishizuka, M., Mikami, M., Leys, J. F., & Huang, N. (2020). Dependency of particle size distribution at dust emission on friction velocity and atmospheric boundary-layer stability. *Atmospheric Chemistry and Physics*, *20*, 12939–12953. https://doi.org/10.5194/acp-20-12939-2020
Sherman, D. J. (2020). Understanding wind-blown sand: Six vexations. *Geomorphology*, *366*, 107193. https://doi.org/10.1016/j.geomorph.2020.107193
Sow, M., Alfaro, S. C., Rajot, J. L., & Marticorena, B. (2009). Size resolved dust emission fluxes measured in Niger during 3 dust storms of the AMMA experiment. *Atmospheric Chemistry and Physics*, *9*, 3881–3891. https://doi.org/10.5194/acp-9-3881-2009
Stout, J. E. (1990). Wind erosion within a simple field. *Transactions of the American Society of Agricultural Engineers*, *33*, 1597–1600. https://doi.org/10.13031/2013.31513
Stout, J. E., & Zobeck, T. M. (1996). The Wolfforth field experiment: A wind erosion study. *Soil Science*, *161*, 616–632. https://doi.org/10.1097/00010694-199609000-00006
TSI Inc. (2012). *Inlet aspiration efficiency of the DustTrak environmental enclosure model 8535, application note ITI-060 (A4)*. TSI Inc.
Webb, N. P., Chappell, A., Edwards, B. L., McCord, S. E., Van Zee, J. W., Cooper, B. F., et al. (2019). Reducing sampling uncertainty in aeolian research to improve change detection. *Journal of Geophysical Research: Earth Surface*, *124*, 1366–1377. https://doi.org/10.1029/2019jf005042
Webb, N. P., Chappell, A., Strong, C. L., Marx, S. K., & McTainsh, G. H. (2012). The significance of carbon-enriched dust for global carbon accounting. *Global Change Biology*, *18*, 3275–3278. https://doi.org/10.1111/j.1365-2486.2012.02780.x
Webb, N. P., Galloza, M. S., Zobeck, T. M., & Herrick, J. E. (2016). Threshold wind velocity dynamics as a driver of aeolian sediment mass flux. *Aeolian Research*, *20*, 45–58. https://doi.org/10.1016/j.aeolia.2015.11.006
Webb, N. P., & Strong, C. L. (2011). Soil erodibility dynamics and its representation in wind erosion and dust emission models. *Aeolian Research*, *3*, 165–179. https://doi.org/10.1016/j.aeolia.2011.03.002
Wolfe, S. A., & Nickling, W. G. (1993). The protective role of sparse vegetation in wind erosion. *Progress in Physical Geography*, *17*, 50–68. https://doi.org/10.1177/030913339301700104
Ziegler, N. P., Webb, N. P., Chappell, A., & LeGrand, S. L. (2020). Scale invariance of albedo-based wind friction velocity. *Journal of Geophysical Research: Atmospheres*, *125*, e2019JD031978. https://doi.org/10.1029/2019jd031978
Zobeck, T. M. (1991). Abrasion of crusted soils: Influence of abrader flux and soil properties. *Soil Science Society of America Journal*, *55*, 1091–1097. https://doi.org/10.2136/sssaj1991.03615995005500040033x
Zobeck, T. M., & Van Pelt, R. S. (2006). Wind-induced dust generation and transport mechanics on a bare agricultural field. *Journal of Hazardous Materials*, *132*(1), 26–38. https://doi.org/10.1016/j.jhazmat.2005.11.090